iJRASET
International Journal For Research in Applied Science and Engineering Technology

INTERNATIONAL JOURNAL FOR RESEARCH

IN APPLIED SCIENCE & ENGINEERING TECHNOLOGY

Volume: 5 **Issue:** XI **Month of publication:** November 2017

DOI: http://doi.org/10.22214/ijraset.2017.11119

www.ijraset.com

Call: 08813907089 | E-mail ID: ijraset@gmail.com

International Journal for Research in Applied Science & Engineering Technology (IJRASET)
ISSN: 2321-9653; IC Value: 45.98; SJ Impact Factor:6.887
Volume 5 Issue X1, November 2017- Available at www.ijraset.com

Static Bending Behavior of FG-CNT Reinforced Composite Plates Using Higher Order Shear Deformation Theory

Vijaya Lakshmi Akurathi[1], J. Suresh Kumar[2]
[1, 2] *Department of Mechanical Engineering, JNTUH College of Engineering, J.N.T.University, Hyderabad*

Abstract: ***The analytical formulations and solutions for the bending behavior of simply supported functionally graded carbon nanotube reinforced composite plates (FG-CNT Plates) are presented in this paper. Higher Order Shear Deformation Theory (HSDT) without enforcing zero transverse shear stresses on the top and bottom surfaces of the plate is used for the analysis. Two types of carbon nanotube (CNT) distributions are analyzed in this investigation. It is assumed that through the thickness, the material properties of the plate are varied. The governing equations of motion and boundary conditions are derived based on the principle of virtual work. Solutions are obtained for FG- CNT Plates in closed-form using Navier's technique. The deflections and stresses are shown for simply supported boundary conditions. The effect of side-to-thickness ratio, aspect ratio, the volume fraction, and through-the-thickness on the deflections and stresses are studied in this paper. The obtained results are compared with the available FSDT solutions in the literature for deflections. This research also shows that the volume fraction of CNT has little effect on stresses. A computer program in C is developed for determining deflections and stresses.***
Keywords: Static Bending Behavior, FG-CNT Plates, Effective Material Properties, HSDT, Navier's Method.

I. INTRODUCTION

In 1987, Niino and co-workers proposed initially the concept of functionally graded materials(FGMs) [1]. Functionally graded materials available in nature as bones, teeth etc. [2], that are designed by nature to meet their expected service requirements. This concept is reproduced from nature to solve an engineering problem. Functionally graded materials (FGMs) are gaining interest from researchers during recent years since these are advanced materials which show improvement in properties like thermal, mechanical, light-weight, dimensional stability, barrier properties, flame retardancy, heat resistance and electrical conductivity [3-4]. Initially, FGMs were utilized as thermal barrier materials for aerospace structural applications and fusion reactors [5]. FGMs also found significance in structural components functioning under very high-temperature environments [6]. As the content of reinforcement in FGMs varies gradually in some direction leads to gradation in properties through the thickness of plate thus eliminates interface problems and reduces stress concentrations [7]. The carbon nanotubes have great stiffness and axial strength due to carbon-carbon Sp2 bonding. They are the excellent stiff materials [8] with Young's modulus of 1.4 TPa and tensile strength well above 100 GPa. The CNT reinforced functionally graded composite materials(FGCM) having a wide variety of applications in different technological areas such as aerospace, defence, energy, automobile, medicine, structural and chemical industry [9].

Researchers have been proposed a variety of plate theories to interpret the behavior of plates earlier. It is helpful to discuss some developments in plate theory and their applications in the analysis of plates. The Classical Laminate Plate Theory (CLPT) [10], introduces the coupling phenomenon between in-plane stretching and transverse bending. The FSDTs developed by Reissner's [11] and Mindlin's [12] constitute the transverse shear deformation effect through the thickness of the plate, that requires a shear correction factor which is difficult to determine correctly. But FSDT provides an adequate interpretation of response for thin to moderately thick plates. A new sinusoidal shear deformation theory is developed without using the shear correction factor for bending, buckling and vibration of FG plates[13]. In order to overcome the drawbacks of FSDT, HSDTs were developed which involved higher order terms in the displacements in the thickness coordinate. Remarkable among them are Reddy [14], Zenkour [15-17], Kant and Co-workers [18-23], Kadkhodayan [24], Matsunaga [25,26], Xiang [27] and Ferreira [28]. The buckling, vibration, linear and nonlinear bending behaviors of FG-CNT reinforced composite structures have drawn much concentration from researchers [29] because of the capability of FG-CNT reinforced composites to control deformation, dynamic response, wear, corrosion etc. and potential to design for different complex environments. Application of some of the theories for the analysis of FG-CNT reinforced composite plates is reviewed here from literature.

Hui-Shen Shen [30], presents the nonlinear bending of simply supported, functionally graded plates reinforced by single-walled carbon nanotubes (SWCNTs) subjected to transverse uniform or sinusoidal load in thermal environments. Applying a higher order shear deformation plate theory with a von Kármán-type of kinematic nonlinearity and include thermal effects shows that the load-bending moment curves of the plate can be notably increased as a result of gradation in reinforcement. Based on the FSDT, Zhu et al. [31] carried out bending and free vibration analyses of thin-to-moderately thick composite plates reinforced by single-walled carbon nanotubes. Numerical results are found with the aid of finite element code. By comparing plates with different distributions of CNT they found CNTs distributed close to top and bottom surfaces are more efficient than those distributed near the mid-plane for increasing the stiffness of the plates. Based on 3D theory of elasticity Alibeigloo and Liew [32] presented the behavior of FG-CNTRC rectangular plate subjected to thermo-mechanical loads under bending. A further static analysis of FG-CNTRC plate embedded in thin piezoelectric layers subjected to uniform mechanical load was conducted by Alibeigloo using the same theory [33] that discuss the effect of volume fraction of CNT, length to thickness ratio, piezoelectric layer thickness ratio.

M. Mohammadimehr, M. Salemi, B. Rousta Navi [34] investigated bending, buckling and free vibration behaviors of micro-composite plate reinforced by FG-SWCNT under hydro-thermal environments using third-order shear deformation theory (TSDT) and modified strain gradient theory (MSGT). This investigation reveals that the critical buckling load and natural frequency for MSGT are more than that of for classic theory (CT) and modified coupled stress theory (MCST), and vice versa for the deflection. Using HSDT theory, L.W. Zhang et al.[35] studied the vibration analysis of FG-CNT reinforced composite plates subjected to in-plane loads based on State-space Levy method. Apart from natural frequencies and mode shapes, the critical in-plane loads for the buckling of different FG-CNT plates are also calculated. Free vibration characteristics of FG-SWCNT reinforced triangular plates are presented by L.W. Zhang et al.[36] using the FSDT and element-free IMLS-Ritz method. Thermal and postbuckling behaviors are presented by Shen H S and Zhang C L [37] for functionally graded nano composite plates reinforced by SWCNTs subjected to in-plane temperature variation. Z.X. Lei, K.M. Liew, J.L. Yu [38] did the buckling analysis of FG-CNT reinforced plates under various loads, using the element-free kp-Ritz method. Most of the above discussed theories do not account for transverse shear stresses on the top and bottom surfaces of the plate. This must be considered while modeling of the FG-CNT Plates, because of the transverse shear stresses and strains are not zero, when the FG-CNT Plates used in aerospace structures that are subjected to transverse load/pressure.

In the present study, static analysis of FG-CNT Plates using HSDT is carried out without constraining zero transverse shear stress on the top and bottom surfaces of the plate. The governing equations and boundary conditions are derived by employing the principle of virtual work. The solution is obtained using Navier method for plates under transverse sinusoidal load for simply supported boundary conditions. The present study results are compared with the available solutions in the literature for deflections, from which it can be concluded that the proposed theory results are varied from the published ones because of the difference in type of load taken and the displacement model taken. The effect of side-to-thickness ratio, aspect ratio, the volume fraction of CNT, and through-the-thickness on the deflections and stresses are studied.

II. THEORETICAL FORMULATION

In formulating the higher-order shear deformation theory, FG-CNT reinforced composite plates with two different distributions of CNT are considered. The length, width and thickness of the FG-CNT reinforced composite plate are a, b and h respectively. FG-CNT reinforced composite plates with these CNT configurations are displayed in Fig. 1. One is uniform distribution of CNT denoted by UD and other is FGX for which both the top and bottom surfaces of the plate are CNT-rich.

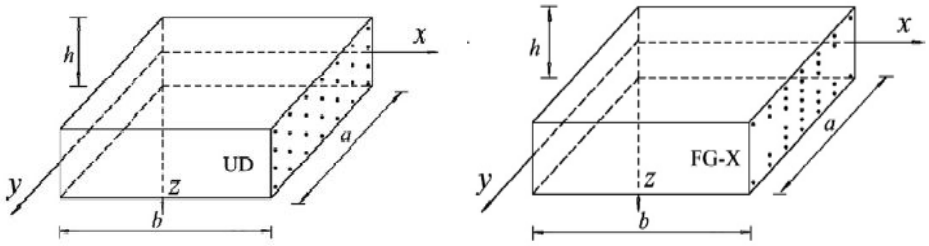

Fig. 1 Types of distribution for the CNTs in the FG-CNT plate.[31]

The volume fractions of the two distribution types are expressed as follows:

$V_{CNT}(z) = V^*_{CNT}$,(UD)

(1)

$V_{CNT}(z) = \frac{4|z|}{h} V^*_{CNT}$, (FGX)

where, $V^*_{CNT} = \frac{m_{CNT}}{m_{CNT}+(\rho^{CNT}/\rho^m)-(\rho^{CNT}/\rho^m)m_{CNT}}$

in which m_{CNT} is the mass fraction of the CNTs, and ρ^m and ρ^{CNT} are densities of the matrix and CNTs.

The effective Young's moduli and Poisson's ratio along the thickness are calculated by:

$$E_{11} = \eta_1 V_{CNT}(z) E_{11}^{CNT} + V_m(z) E^m$$

$$\frac{\eta_2}{E_{22}} = \frac{V_{CNT}(z)}{E_{22}^{CNT}} + \frac{V_m(z)}{E^m}$$

(2)

$$\frac{\eta_3}{G_{12}} = \frac{V_{CNT}(z)}{G_{12}^{CNT}} + \frac{V_m(z)}{G^m}$$

$$\upsilon_{12} = V^*_{CNT}\upsilon_{12}^{CNT} + V_m\upsilon^m$$

$$\upsilon_{21} = \upsilon_{12}E_{22}/E_{11}$$

$$\rho_0 = V_{CNT}(z)\rho^{CNT} + V_m(z)\rho^m$$

where E_{11}^{CNT} , E_{22}^{CNT} and G_{12}^{CNT} are the elastic and shear moduli of the transversely isotropic CNT. E^m and G^m are the corresponding properties of the isotropic matrix. CNT efficiency parameters η_1 ,η_2 *and* η_3 are introduced to account for load transfer between the CNT and polymeric phases as the load transfer between the CNT and matrix is less than perfect. V_{CNT} *and* V_m are the volume fractions of the CNT and matrix, and their sum must be equal to 1, that is $V_{CNT} + V_m = 1$.

A. Displacement Model

A 3D-elasticity plate problem is approximated as a 2D one by expanding the displacement components u, v and w which are function of (x, y, z) at any point in the plate in terms of the thickness coordinate. The elasticity solution demonstrates that through the plate thickness the transverse shear stress varies parabolic ally which demands the use of a displacement field, in which the in-plane displacements are expanded as cubic functions of the thickness coordinate. The displacement field which assumes w constant through the plate thickness thus setting $\varepsilon_z = 0$ is expressed as: [39]

$$u(x,y,z) = u_o(x,y) + z\theta_x(x,y) + z^2u_o^*(x,y) + z^3\theta_x^*(x,y)$$
$$v(x,y,z) = v_o(x,y) + z\theta_y(x,y) + z^2v_o^*(x,y) + z^3\theta_y^*(x,y)$$
$$w(x,y,z) = w_o(x,y)$$

(3)

where u_0 , v_0, w_0 denote the mid-plane displacements of a point (x, y) and θ_x, θ_y are the rotations of the normal to the mid-plane about y and x axes, respectively. The parameters u_0^*, v_o^*, θ_x^*, θ_y^* are the corresponding higher-order deformation terms.

B. Elastic Stress-Strain Relations

Since $_z = 0$, the transverse normal stress $_z$, although not zero identically, does not appear in the virtual work statement and hence in the equations of motion. Consequently, it amounts to neglecting the transverse normal stress. Thus we have, in theory, a case of plane stress [40]. For an FG-CNT reinforced composite laminate, the plane stress reduced elastic constants and the transformed plane stress reduced elastic constants will be same i.e., $C_{ij} = Q_{ij}$. The constitutive relations for FG-CNT materials can be written as:

$$\begin{Bmatrix}\sigma_x\\ \sigma_y\\ \tau_{xy}\end{Bmatrix} = \begin{bmatrix}Q_{11} & Q_{12} & 0\\ Q_{12} & Q_{22} & 0\\ 0 & 0 & Q_{33}\end{bmatrix}\begin{Bmatrix}\varepsilon_x\\ \varepsilon_y\\ \gamma_{xy}\end{Bmatrix}$$

$$\begin{Bmatrix}\tau_{yz}\\ \tau_{xz}\end{Bmatrix} = \begin{bmatrix}Q_{44} & 0\\ 0 & Q_{55}\end{bmatrix}\begin{Bmatrix}\gamma_{yz}\\ \gamma_{xz}\end{Bmatrix} \qquad (4)$$

where, σ_x , σ_y, τ_{xy} , τ_{yz} , τ_{xz} are the stresses and ε_x , ε_y, γ_{xy} , γ_{yz} , γ_{xz} are the strains with respect to the axes. Q_{ij} are the plane stress reduced elastic constants in the plate axes that vary through the plate thickness and are given by:

$$Q_{11} = \frac{E_{11}}{(1-\upsilon_{12}\upsilon_{21})}, \quad Q_{22} = \frac{E_{22}}{(1-\upsilon_{12}\upsilon_{21})}, Q_{33} = G_{12},$$

$$Q_{12} = \frac{\upsilon_{21}E_{11}}{(1-\upsilon_{12}\upsilon_{21})}, \quad Q_{44} = G_{23}, Q_{55} = G_{13}$$

where,

E_{ii} = Young's modulus of elasticity in the i direction.

υ_{ij} = Poisson's ratios that give strain in the j direction due to stress in the i direction.

G_{ij} = shear moduli , and these are computed using Eq. (2).

C. Governing Equations of Motion

The energy principle states that the work done by actual forces in moving through virtual displacements, that are consistent with the geometric constraints of a body is set to zero to obtain the equations of motion. This principle is useful in deriving governing equations, boundary conditions and obtaining approximate solutions by virtual methods. Energy principles provide another means to obtain the governing equations and their solutions. In the current study, the principle of virtual work is used to derive the equations of motion for FG-CNT plates. The governing equations of higher-order theory for the displacement model given in Eq. (3) will be derived using the dynamic version of the principle of virtual displacements, i.e.

$$\int_0^T (\delta U + \delta V - \delta K)\, dt = 0 \qquad (5)$$

where δU, δV, δK are virtual strain energy, virtual work done by applied forces and virtual kinetic energy respectively.

$$\delta U = \int_A \left\{ \int_{-h/2}^{h/2} \left[\sigma_x \delta\varepsilon_x + \sigma_y \delta\varepsilon_y + \tau_{xy}\delta\gamma_{xy} + \tau_{xz}\delta\gamma_{xz} + \tau_{yz}\delta\gamma_{yz}\right] dz \right\} dx\, dy$$

$$\delta V = \int_{-\frac{h}{2}}^{\frac{h}{2}} q\,\delta w_0\, dx dy$$

$$\delta K = \int_A \left\{ \int_{-h/2}^{h/2} \rho_0 \left[\left(\dot{u}_0 + Z\dot{\theta}_x + Z^2\dot{u}_0^* + Z^3\dot{\theta}_x^*\right)\left(\delta\dot{u}_0 + Z\delta\dot{\theta}_x + Z^2\delta\dot{u}_0^* + Z^3\delta\dot{\theta}_x^*\right) + \left(\dot{v}_0 + Z\dot{\theta}_y + Z^2\dot{v}_0^* + Z^3\dot{\theta}_y^*\right)\left(\delta\dot{v}_0 + Z\delta\dot{\theta}_y + Z^2\delta\dot{v}_0^* + Z^3\delta\dot{\theta}_y^*\right) + \dot{w}_0\delta\dot{w}_0 \right] dz \right\} dx dy$$

where,

q = transverse load on the surface of the plate.

ρ_0 = Density of plate material

On substituting for δU, δV and δK into the virtual work statement in Eq. (5) and integrating through the thickness, integrating by parts and collecting the coefficients of each of virtual displacements δu_o δv_0, δw_0, $\delta\theta_x$, $\delta\theta_y$, δu_0^*, δv_0^*, $\delta\theta_x^*$, $\delta\theta_y^*$ in a domain of any differentiation the statement of virtual work is obtained as governing equations of motion.

$$\delta u_0 : \frac{\partial N_x}{\partial x} + \frac{\partial N_{xy}}{\partial y} = I_1\ddot{u}_0 + I_2\ddot{\theta}_x + I_3\ddot{u}_0^* + I_4\ddot{\theta}_x^*$$

$$\delta v_0 : \frac{\partial N_y}{\partial y} + \frac{\partial N_{xy}}{\partial x} = I_1 \ddot{v}_0 + I_2 \ddot{\theta}_y + I_3 \ddot{v}_0^* + I_4 \ddot{\theta}_y^*$$

$$\delta w_0 : \frac{\partial Q_x}{\partial x} + \frac{\partial Q_y}{\partial y} + q = I_1 \ddot{w}_0$$

$$\delta\theta_x : \frac{\partial M_x}{\partial x} + \frac{\partial M_{xy}}{\partial y} - Q_x = I_2 \ddot{u}_0 + I_3 \ddot{\theta}_x + I_4 \ddot{u}_0^* + I_5 \ddot{\theta}_x^*$$

$$\delta\theta_y : \frac{\partial M_y}{\partial y} + \frac{\partial M_{xy}}{\partial x} - Q_y = I_2 \ddot{v}_0 + I_3 \ddot{\theta}_y + I_4 \ddot{v}_0^* + I_5 \ddot{\theta}_y^*$$

$$\delta u_0^* : \frac{\partial N_x^*}{\partial x} + \frac{\partial N_{xy}^*}{\partial y} - 2S_x = I_3 \ddot{u}_0 + I_4 \ddot{\theta}_x + I_5 \ddot{u}_0^* + I_6 \ddot{\theta}_x^*$$

$$\delta v_0^* : \frac{\partial N_y^*}{\partial y} + \frac{\partial N_{xy}^*}{\partial x} - 2S_y = I_3 \ddot{v}_0 + I_4 \ddot{\theta}_y + I_5 \ddot{v}_0^* + I_6 \ddot{\theta}_y^* \qquad (6)$$

$$\delta\theta_x^* : \frac{\partial M_x^*}{\partial x} + \frac{\partial M_{xy}^*}{\partial y} - 3Q_x^* = I_4 \ddot{u}_0 + I_5 \ddot{\theta}_x + I_6 \ddot{u}_0^* + I_7 \ddot{\theta}_x^*$$

$$\delta\theta_y^* : \frac{\partial M_y^*}{\partial y} + \frac{\partial M_{xy}^*}{\partial x} - 3Q_y^* = I_4 \ddot{v}_0 + I_5 \ddot{\theta}_y + I_6 \ddot{v}_0^* + I_7 \ddot{\theta}_y^*$$

The force resultants and moment resultants can be related to the total strains by the following matrix:

$$\begin{Bmatrix} N \\ N^* \\ -- \\ M \\ M^* \\ -- \\ Q \\ Q^* \end{Bmatrix} = \left[\begin{array}{c|c|c} A & B & 0 \\ \hline B^t & D_b & 0 \\ \hline 0 & 0 & D_s \end{array}\right] \begin{Bmatrix} \varepsilon_0 \\ \varepsilon_0^* \\ -- \\ K \\ K^* \\ -- \\ \phi \\ \phi^* \end{Bmatrix} \qquad (7)$$

Where,

N, N^*, M, M^*, Q, Q^* are called the in-plane force resultants, moment resultants and transverse force resultants respectively. They can be written in matrix form as follows.

$N = [N_x \;\; N_y \;\; N_{xy}]^t$; $N^* = [N_x^* \;\; N_y^* \;\; N_{xy}^*]^t$

$M = [M_x \;\; M_y \;\; M_{xy}]^t$; $M^* = [M_x^* \;\; M_y^* \;\; M_{xy}^*]^t$

$Q = [Q_x \;\; Q_y]^t$; $Q^* = [S_x \;\; S_y \;\; Q_x^* \;\; Q_y^*]^t$

$\varepsilon_0 = [\varepsilon_{x0} \;\; \varepsilon_{y0} \;\; \varepsilon_{xy0}]^t$; $\varepsilon_0^* = [\varepsilon_{x0}^* \;\; \varepsilon_{y0}^* \;\; \varepsilon_{xy0}^*]^t$ $k = [k_x \;\; k_y \;\; k_{xy}]^t$; $k^* = [k_x^* \;\; k_y^* \;\; k_{xy}^*]^t$ $\phi = [\phi_x \;\; \phi_y]^t$; $\phi^* = [\varepsilon_{xz0} \;\; \varepsilon_{yz0} \;\; \phi_x^* \;\; \phi_y^*]^t$

The [A], [B], [D], and [Ds] matrices elements are determined using Eq. (7) and the effective properties of the respective FG-CNT plate from Eq. (2).

III. ANALYTICAL SOLUTIONS

Composite plates are generally classified by referring to the type of support used. The analytical solutions of the governing equations of motion for simply supported FG-CNT plates are dealt here. The plate is assumed to be simply supported in such a way that normal displacement is admissible, but the tangential displacement is not. Solution functions that completely satisfy the

boundary conditions and the transverse mechanical load are considered using Navier method which on substitution in the governing equations of motion yields:

$$[S]_{9X9}\begin{Bmatrix} U_{mn} \\ V_{mn} \\ W_{mn} \\ X_{mn} \\ Y_{mn} \\ U^*_{mn} \\ V^*_{mn} \\ X^*_{mn} \\ Y^*_{mn} \end{Bmatrix} = \begin{Bmatrix} 0 \\ 0 \\ Q_{mn} \\ 0 \\ 0 \\ 0 \\ 0 \\ 0 \\ 0 \end{Bmatrix} \quad (8)$$

Solution of Eq. (8) for each m, n = 1, 2, … gives $U_{mn}, V_{mn}, W_{mn}, X_{mn}, Y_{mn}, U^*_{mn}, V^*_{mn}, X^*_{mn}, Y^*_{mn}$ which can be used to compute u_o, v_o, w_o, θ_x, θ_y ,u^*_o , v^*_o, θ^*_x , θ^*_y .

IV. RESULTS AND DISCUSSION

A. Comparative Studies

In this section, examples are presented and discussed to validate the accuracy of the present higher-order shear deformation theory in predicting the deflections and stresses of a simply supported functionally graded CNT reinforced composite plates. Poly{(m-phenylenevinylene)-co-[(2,5-dioctoxy-p-phenylene) vinylene]} referred as PmPV is selected as the matrix. The material properties of which are as follows:

$E^m = 2.1\ GPa$, $\rho^m = 1.15\frac{g}{cm^3}$, $\vartheta^m = 0.34$

SWCNT (single-walled carbontubes) are taken as the reinforcements and its properties are:

$E_{11}^{CNT} = 5.6466\ TPa$, $E_{22}^{CNT} = 7.0800 TPa$,

$G_{12}^{CNT} = 1.9445\ TPa$, $\upsilon_{12}^{CNT} = 0.175$ and $\rho^{CNT} = 1400\ kg/m^3$ [41].

The values of volume fraction of CNT i.e., V^*_{CNT} and the corresponding CNT efficiency parameters are listed in Table I. It is assumed that the effective shear moduli $G_{13} = G_{23} = G_{12}$ and $\eta_3 = \eta_2$.

TABLE I
EFFICIENCY PARAMETERS OF SWCNTS [34]

V^*_{CNT}	η_1	η_2	η_3
0.11	0.149	0.934	0.934
0.14	0.150	0.941	0.941
0.17	0.149	1.381	1.381

For convenience, the transverse displacement, in-plane and the transverse shear stresses are presented in non-dimensionalized form as:

$\bar{w} = \frac{-w}{h}\left(\frac{a}{2}, \frac{b}{2}\right)$, $\bar{\sigma}_x = \frac{h}{aq}\sigma_x\left(\frac{a}{2}, \frac{b}{2}, \frac{h}{2}\right)$, $\bar{\sigma}_y = \frac{h}{aq}\sigma_y\left(\frac{a}{2}, \frac{b}{2}, \frac{h}{3}\right)$, $\bar{\tau}_{xy} = \frac{h}{aq}\tau_{xy}\left(0,0,-\frac{h}{3}\right)$, $\bar{\tau}_{yz} = \frac{h}{aq}\tau_{yz}\left(\frac{a}{2}, 0, \frac{h}{6}\right)$, $\bar{\tau}_{xz} = \frac{h}{aq}\tau_{xz}\left(0, \frac{b}{2}, 0\right)$ and $\bar{z} = \frac{z}{h}$

TABLE II
COMPARISON OF NON-DIMENSIONALIZED CENTRAL DEFLECTION

V^*_{CNT}	$\frac{a}{h}$	Type of distribution	$\bar{w}$ (Present)	$\bar{w}$ (Ref [31])
0.11	10	UD	0.002510	0.003739
		FGX	0.002141	0.003177
	20	UD	0.024755	0.03628
		FGX	0.018724	0.02701
0.14	10	UD	0.002223	0.003306

		FGX	0.001934	0.002844
	20	UD	0.020627	0.03001
		FGX	0.015813	0.02256
0.17	10	UD	0.001606	0.002394
		FGX	0.001378	0.002012
	20	UD	0.016000	0.02348
		FGX	0.012107	0.01737

Table II shows the comparison of non-dimensional zed central deflection, W for the CNTRC square plate with two cases UD and FG distribution and subjected to sinusoidal transverse load using higher-order theory with non-dimensional zed central deflection, W for the CNTRC square plate with two cases UD and FG distribution and subjected to uniformly distributed load using first order shear deformation theory. Since the governing equation in Ref. [31] is based on the first order shear deformation theory and the load is uniformly distributed so, regardless of the amount of length-to-thickness ratio and volume fraction of CNT constituent, dimensionless transverse displacement of the present formulation is smaller than that of Ref. [31]. As the side-thickness ratio increases the variation of non-dimensional zed central deflection is in good agreement with the published ones (Ref.[31]). And also increase of volume fraction has great influence in the reduction of non-dimensional zed central deflection and this variation also in good agreement with the published ones. The effect of type of distribution of CNT of the FG-CNT plate on the non-dimensional zed deflection also same in the present study and in the literature.

B. Parametric Studies

1) *Effect of Side-to-Thickness Ratio:* The variation of non-dimensional zed displacements and stresses for various side to thickness ratios $\left(\frac{a}{h}\right)$ and for different volume fraction of CNT (V_{CNT}^{*}) for the displacement model are shown in Figures 2 - 7 for two different distributions (UD and FGX) of CNT. Figure 2 shows the variation of center deflection with different volume fractions of CNT (V_{CNT}^{*}) and with different side-to-thickness ratios for different distributions of CNT. It can be observed that the volume fraction of CNT has so much influence on the central deflection of the plates. Only 6% increase in the volume fraction of CNT leads to 35% decrease in central deflection for both the distributions of the CNT reinforced composite. It can also be observed that the deflection of UD-CNT reinforced composite plate is large compared to FGX-CNT reinforced composite because the type of distribution affects the stiffness of the plates. From this it is concluded that the reinforcements distributed near the top and bottom surfaces of more efficient than those distributed near the mid-plane.

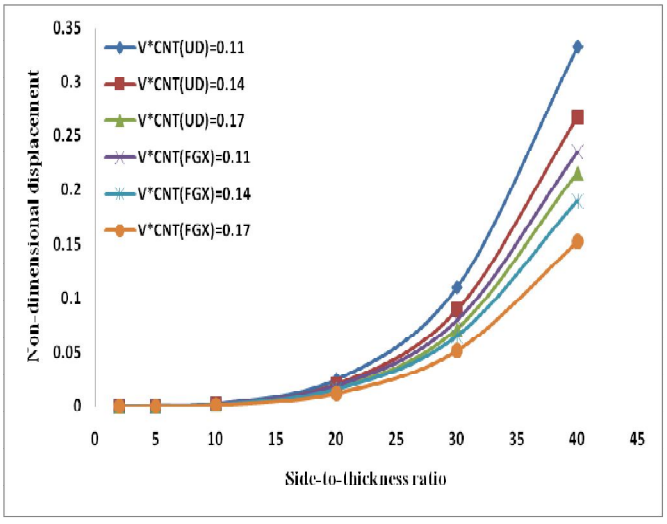

Fig. 2 $(\overline{w})$ as a function of side-to-thickness ratio $(\frac{a}{h})$

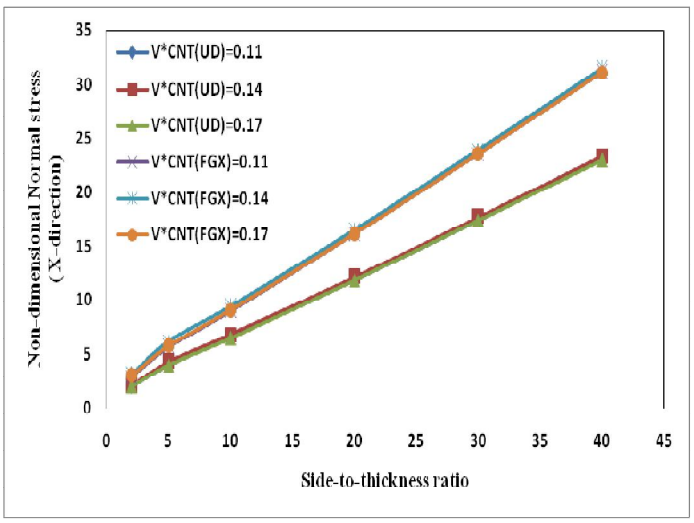

Fig. 3 $(\bar{\sigma}_x)$ as a function of side-to-thickness ratio $(\frac{a}{h})$

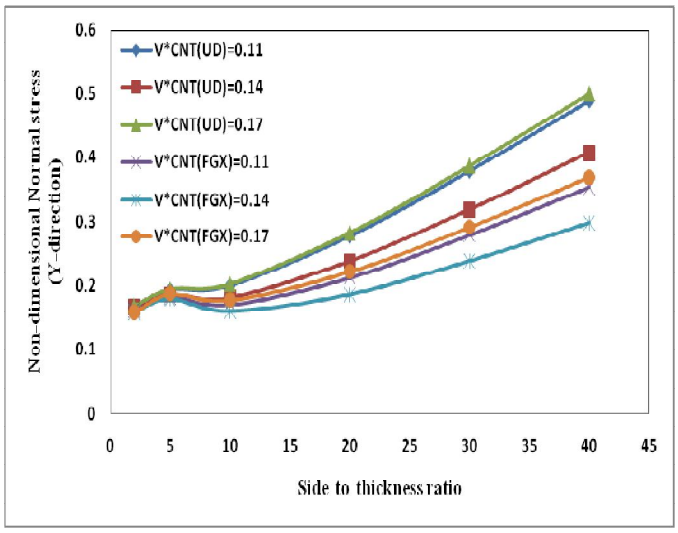

Fig. 4 ($\bar{\sigma}_{yy}$) as a function of side-to-thickness ratio ($\frac{a}{h}$)

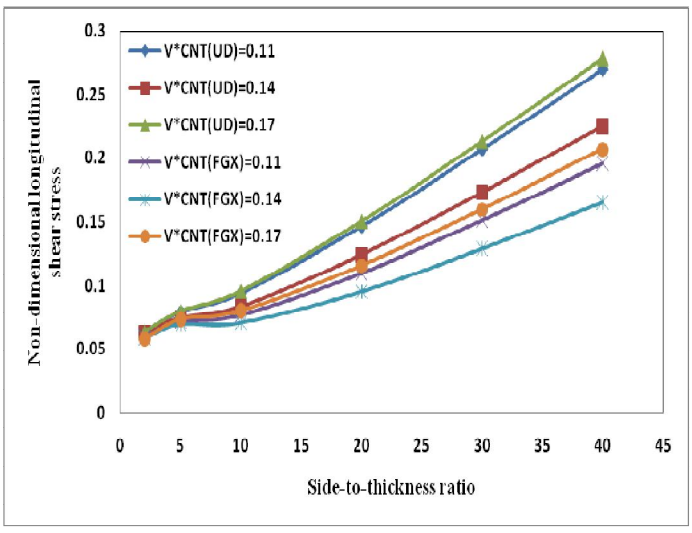

Fig. 5 ($\bar{\sigma}_{xz}$) as a function of side-to-thickness ratio ($\frac{a}{h}$)

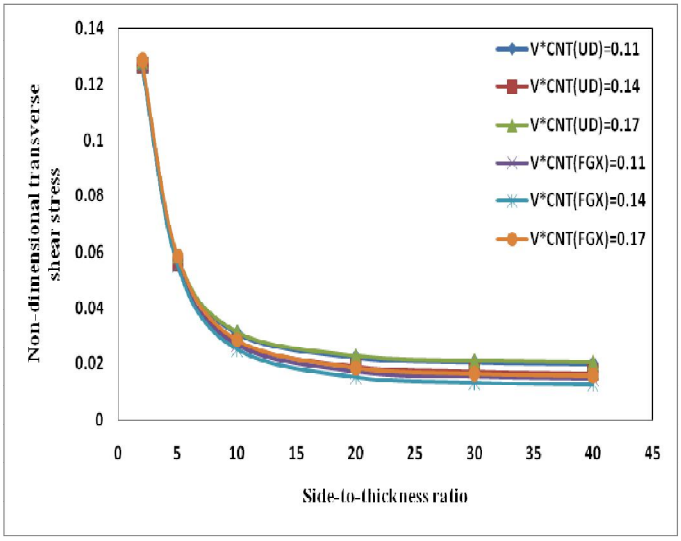

Fig. 6 ($\bar{\sigma}_{yz}$) as a function of side-to-thickness ratio ($\frac{a}{h}$)

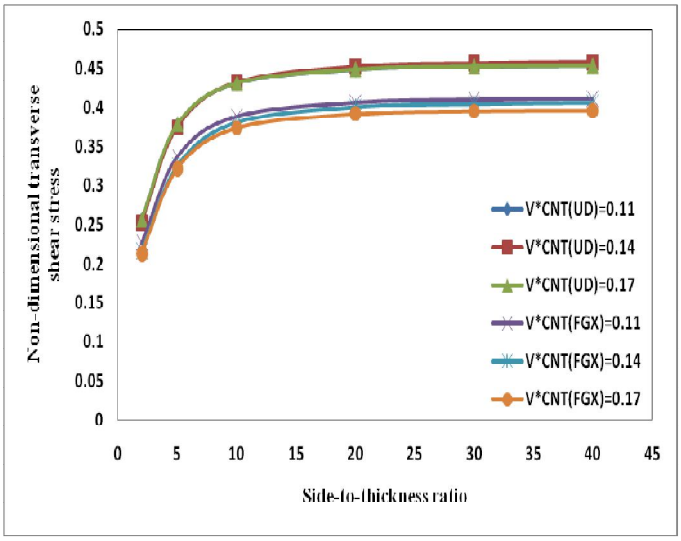

Fig. 7 ($\bar{\sigma}_{yz}$) as a function of side-to-thickness ratio ($\frac{a}{h}$)

2) *Effect of Aspect Ratio:* The effect of aspect ratios $\left(\frac{a}{b}\right)$ and volume fraction of CNT for displacement model for different distributions of CNT on non-dimensionalized displacement and stresses are shown in figures 8 - 13. From figure 8 it can be observed that the central deflection decreases with increase in the aspect ratio and volume fraction of CNT. As stated earlier, small increase in volume fraction of CNT has much effect on reduction of central deflection. Plate with FGX distribution has less central defection compared to UD because of rich distribution of CNT on the top and bottom surfaces of the plate. The volume fraction of CNT doesn't have a remarkable effect on stresses as shown in figures 9 - 13. From figure 9 it can be noticed that with the increase of aspect ratio the in-plane longitudinal stress $\bar{\sigma}_{xx}$ decreases and for a particular aspect ratio, $\bar{\sigma}_{xx}$ is more for FGX distribution of CNT compared to UD. Figure 10 shows that the in-plane normal stress $\bar{\sigma}_{yy}$ increases with the increase of aspect ratio up to an aspect ratio of 2 and then decreases. It can be observed from figure 11 that the longitudinal shear stress $\bar{\sigma}_{xz}$ increases with the increase of aspect ratio up to an aspect ratio of 1.5 and then decreases. Compared to UD, FGX distribution of CNT yields to a less value of $\bar{\sigma}_{xz}$ for a particular aspect ratio. It can be depicted from figure 12 that the transverse shear stress $\bar{\sigma}_{yz}$ increases as the ratio of aspect ratio increases. From figure 13 it can be noted that the transverse shear stress $\bar{\sigma}_{yz}$ decreases as the aspect ratio increases.

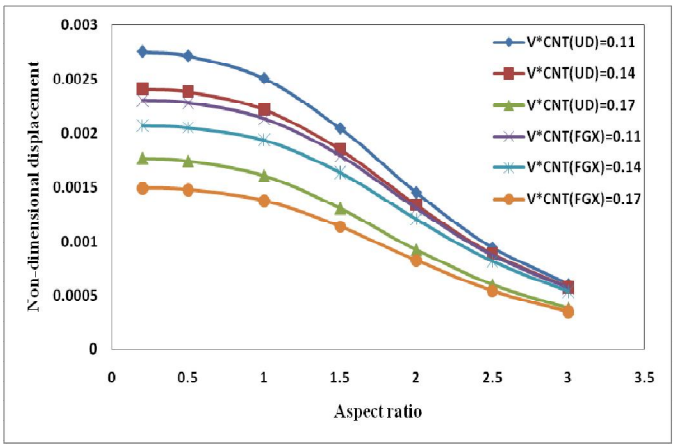

Fig. 8 ($\overline{\square}$) as a function of aspect ratio ($\frac{\square}{\square}$)

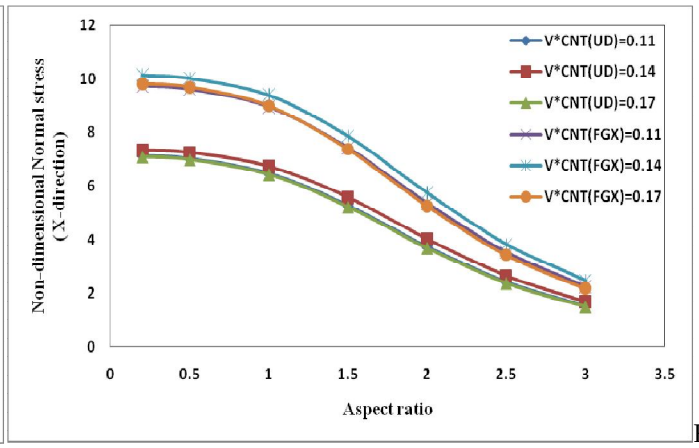

Fig. 9 ($\overline{\square}_{\square}$) as a function of aspect ratio ($\frac{\square}{\square}$)

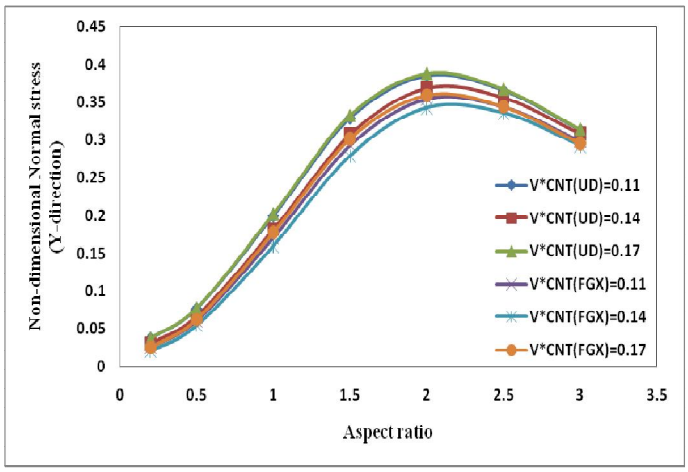

Fig. 10 ($\overline{\square}_{\square}$) as a function of aspect ratio ($\frac{a}{b}$)

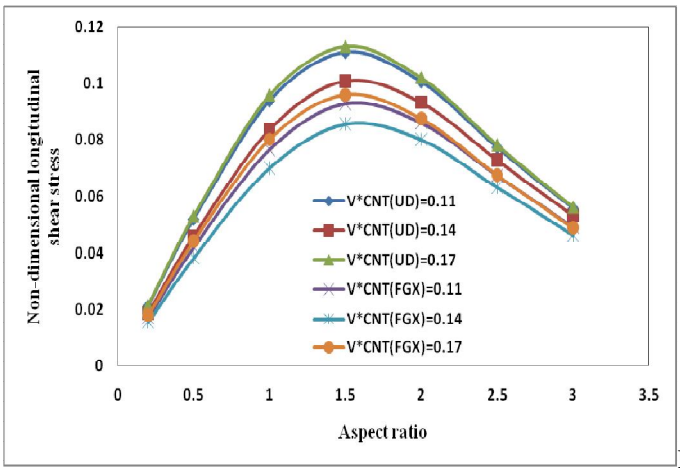

Fig. 11 ($\overline{\square}_{\square\square}$) as a function of aspect ratio ($\frac{a}{b}$)

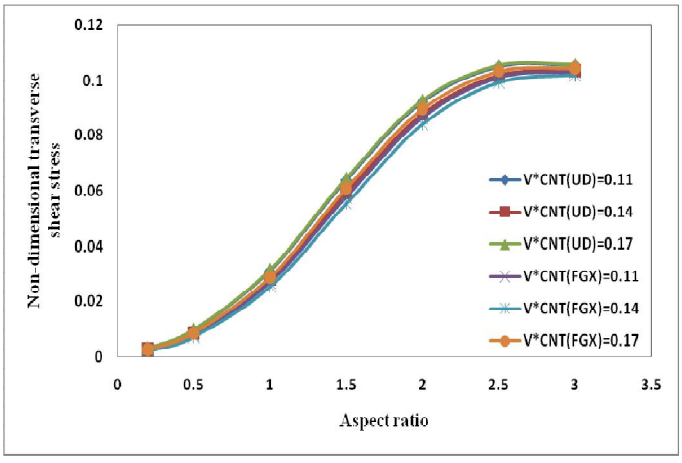

Fig. 12 ($\overline{\square}_{\square\square}$) as a function of aspect ratio ($\frac{a}{b}$)

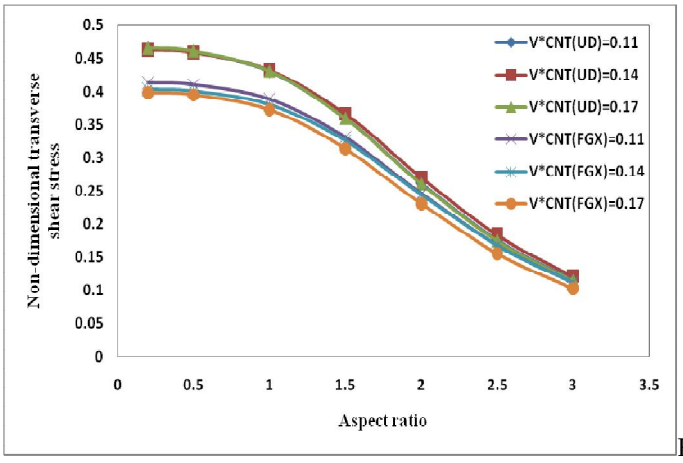

Fig. 13 ($\overline{\square}_{\square\square}$) as a function of aspect ratio ($\frac{a}{b}$)

3) Variation of stresses through-the-thickness: Figures 14 - 18 show the variation of stresses in an FG-CNT reinforced composite plate through the thickness under sinusoidal load. The volume fraction of CNT has very little effect on stresses of FG-CNT reinforced composite plates. As shown in figures 14 - 15, the in-plane longitudinal stress $\overline{\square}_{\square}$ and in-plane normal stress $\overline{\square}_{\square}$ are compressive throughout the plate up to the mid-plane $\overline{\square} = 0$ and then become tensile afterward. The maximum tensile stresses

occur at the top surface of the plate and maximum compressive stresses occur at a point on the bottom of the plate. From figure 16, it can be depicted that the longitudinal shear stress $\bar{\sigma}_{xz}$ gives rise to tensile stress throughout the plate up to the mid-plane $\bar{z} = 0$ and then compressive stress afterward. The maximum compressive stresses occur at the top surface of the plate and maximum tensile stresses occur at a point on the bottom of the plate. The transverse shear stresses $\bar{\sigma}_{xz}$ and $\bar{\sigma}_{yz}$ increases up to mid-plane and then decreases. The maximum value of shear stress occurs at mid-plane for UD and it is near the mid-plane but not exactly at the mid-plane for FGX distribution of CNT. $\bar{\sigma}_{xz}$ and $\bar{\sigma}_{yz}$ have less value for FGX distribution of CNT compared to UD for the particular (z/h) value.

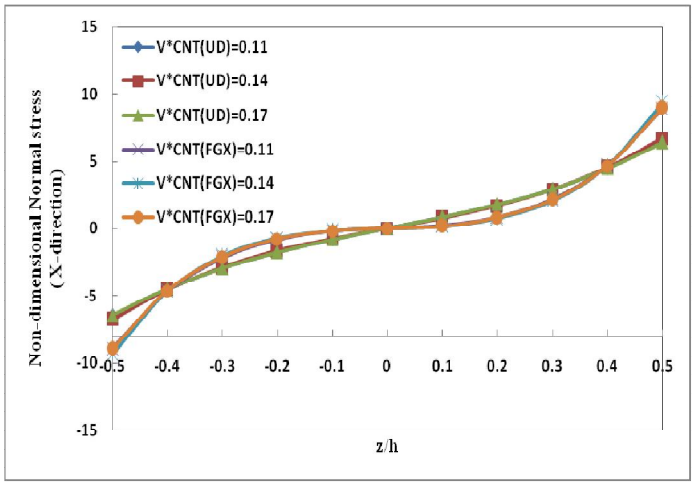

Fig. 14 ($\bar{\sigma}_{x}$) across the thickness of composite plate

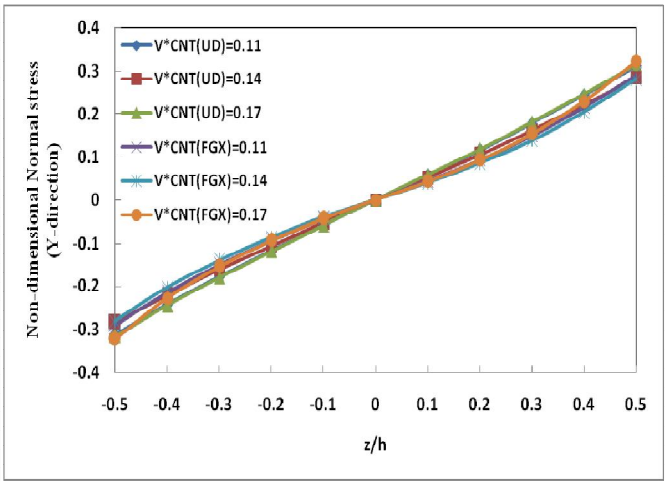

Fig. 15 ($\bar{\sigma}_{y}$) across the thickness of composite plate

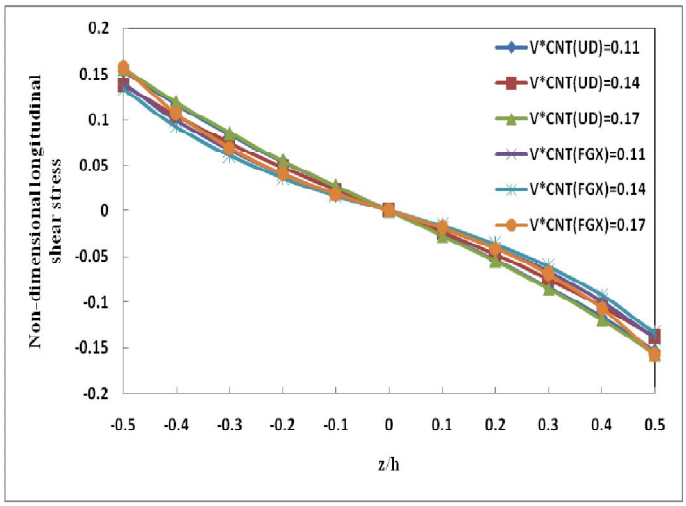

Fig. 16 ($\bar{\sigma}_{xz}$) across the thickness of composite plate

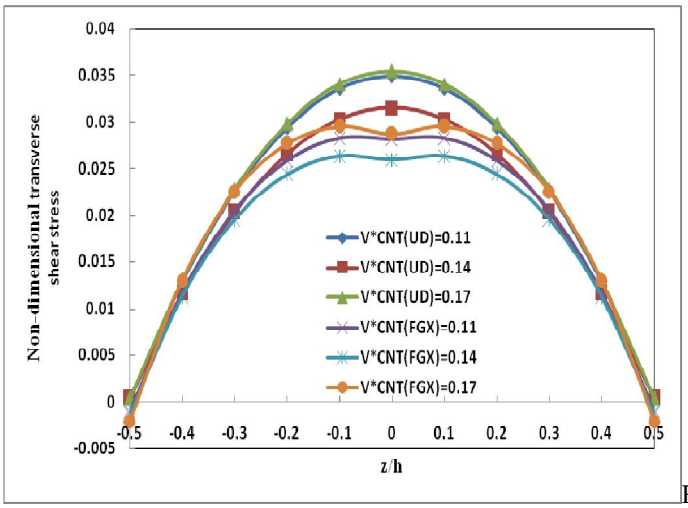

Fig. 17 ($\bar{\sigma}_{yz}$) across the thickness of composite plate

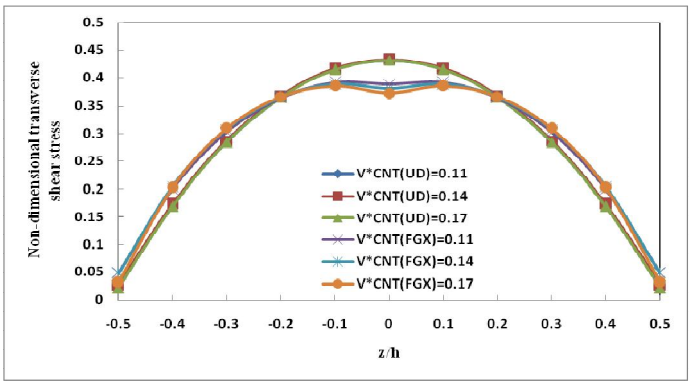

Fig. 18 ($\bar{\square}_{\square\square}$) across the thickness of composite plate

V. CONCLUSIONS

A higher-order shear deformation theory is employed for static bending behavior of simply supported functionally graded CNT reinforced composite plates without enforcing zero transverse shear stresses on the top and bottom surfaces of the plate which eliminates the requirement of shear correction factors. By utilizing the principle of virtual work the governing equations and boundary conditions are derived. The governing equations are solved using Navier's type closed form solution, for FG-CNT plates subjected to sinusoidal load. Comparative studies are carried out to signify the accuracy of the present theory and also between the two types of CNT distributions. The effect of volume fraction of CNT, distribution of CNT and side-to-thickness ratio on deflections for the present study has good consistency with the literature. The analytical formulations and solutions developed herein should be helpful in future studies in the design of FG-CNT plates for various advanced applications. Also, the present research will serve as a benchmark for evaluating the other future plate theories and numerical methods.

REFERENCES

[1] Yamanouchi M., Hirai T., Shiota I.(1990), Proceedings of First International Symposium on Functionally Gradient Materials, FGM Forum, Tokyo, Japan.
[2] R. Knoppers, J. W. Gunnink, J. Van den Hout, and W. Van Vliet, The reality of functionally graded material products, TNO Science and Industry, The Netherlands, pp 38-43.
[3] Pindera, M.-J., Aboudi, J, Glaeser, A M., and Arnold, S. M (1997), Use of Composites in Multi-Phased and Functionally Graded Materials, Composites, Part B 28, pp. 1-175.
[4] Suresh, S., and Mortensen (1998), A, Fundamentals of Functionally Graded Materials, 10M Communications, London.
[5] Pindera, M.-J., Arnold, S. M, Aboudi, J, and Hui, D.(1994), Use of Composites in Functionally Graded Materials, Composites Eng.4, pp. 1-145.
[6] Pindera, M.-J., Aboudi, J, Arnold, S. M, and Jones, W. F.(1995), Use of Composites in Multi-Phased and Functionally Graded Materials, Composites Eng., 5, pp. 743-974.
[7] M. S. EL-Wazery, A. R. EL-Desouky(2015), A review on Functionally Graded Ceramic-Metal Materials, Environ. Sci. 6 (5) 1369-1376.
[8] Treacy, M. J., and Ebberse, W.(1996), Exceptionally High Young's Modulus Observed for Individual Carbon Nanotubes, Nature, Vol. 381, pp. 678.
[9] Udupa G, Rao SS, Gangadharan KV (2012) Future application of Carbon Nanotube reinforced Functionally Graded Composite Materials. Proceedings of IEEE-International conference on Advances in Engineering, Science and Management.
[10] E. Reissner and Y.Stavsk (1961), Bending and stretching of certain types of heterogeneous aelotropic elastic plates. ASME J ApplMech, Vol. 28 402-428.
[11] E. Reissner (1945),The effect of transverse shear deformation on the bending of elastic plates. ASME J ApplMech, Vol. 12 No. 2, 69-77.
[12] R. D Mindlin (1951), Influence of rotary inertia and shear on flexural motions of isotropic, elastic plates. ASME J ApplMech, Vol. 18 31-38.
[13] Huu-Tai Thai and ThucP.Vo (2013), A new sinusoidal shear deformation theory for bending, buckling, and vibration of functionally graded paltes. Appl Math Model,Vol. 37 3269-3281.
[14] J.N. Reddy and C.D. Chin (1998), Thermomechanical analysis of functionally graded cylinders and plates. J Therm stress, Vol. 21 No.6, 593-626.
[15] A.M. Zenkour (2005), A comprehensive analysis of functionally graded sandwich plates:Part-1-Deflection and stresses. Int J Solids Struct, Vol. 42 No. 18-19, 5224-5242.
[16] A.M. Zenkour (2005), A comprehensive analysis of functionally graded sandwich plates:Part-2-Buckling and free vibration. Int J Solids Struct, Vol. 42 No. 18-19, 5243-5258.
[17] A.M. Zenkour (2006) ,Generalized shear deformation theory for bending analysis of functionally graded plates. Appl Math Model,Vol. 30 No. 1, 67-84.
[18] T. Kant, D.R.J.Owen, and O. C Zienkiewicz (1982),A refined higher order C0 plate element. Computstruct, Vol. 15 No. 2, 177-183.
[19] B.N.Pandya, and T. Kant (1988), Higher-order shear deformable theories for flexure of sandwich plates-finite element evaluations. Int J solids Struct, Vol. 24 No. 12, 1267-1286.
[20] B.N.Pandya, and T. Kant (1988), Finite element analysis of laminated composite plates using a higher order displacement model. Compos SciTechnol,Vol. 32, No. 2, 137-155.
[21] T. Kant, and K. Swaminathan (2002), Analytical solutions for the static analysis of laminated composite and sandwich plates based on higher order refined theory. Composite struct, Vol. 56 No. 4, 329-344.

[22] T. Kant, and K. Swaminathan (2001), Analytical solutions for free vibration analysis of laminated composite and sandwich plates based on higher order refined theory. compositestruct, Vol. 53 No. 1, 73-85.
[23] Garg Ajay Kumar, KhareRakesh Kumar, Kant Tarun (2006), Higher order closed form solutions for free vibration of laminated composite and sandwich shells. J Sandwich struct Mater, Vol. 8 No. 3, 205-235.
[24] M. E. Golmakani, and M. Kadkhodayan (2011), Nonlinear bending analysis of annular FGM plates using higher order shear deformation plate theories. Composite struct,Vol. 93 973-982.
[25] Hiroyuki Matsunaga (2008), Free vibration and stability of functionally graded plates according to a 2-D higher-order deformation theory. Composite struct, Vol. 82 499-512.
[26] Hiroyuki Matsunaga (2009), Stress analysis of functionally graded plates subjected to thermal and mechanical loadings. Composite struct, Vol. 87 344-357.
[27] Song Xiang and Gui-wen Kang (2013), A nth-order shear deformation theory for the bending analysis on the functionally graded plates. European Journal of Mechanics A/Solids,Vol. 37 336-343.
[28] A.M.A. Neves, A.J.M. Ferreira, E.Carrera, M.Cinefra, C.M.C.Roque, R.M.N.Jorge, and C.M.M. Soares (2013), Free vibration analysis of functionally graded shells by a higher-order shear deformation theory and radial basis functions collocation, accounting for through-the-thickness deformations. European Journal of Mechanics A/Solids, Vol. 37 24-34.
[29] Liew KM, Lei ZX and Zhang L W (2015) Mechanical analysis of functionally graded carbon nanotube reinforced composites: A review. Compos. Struct. 120 90-97
[30] Hui-Shen Shen(2009), Nonlinear bending of functionally graded carbon nanotube-reinforced composite plates in thermal environments, Composite Structures 91 9–19.
[31] Zhu P, Lei ZX, Liew KM.(March 2012), Static and free vibration analyses of carbon nanotube-reinforced composite plates using finite element method with first order shear deformation plate theory. Compos Struct. Volume 94, Issue 4, Pages 1450–1460.
[32] Alibeigloo A, Liew KM. (2013), Thermoelastic analysis of functionally graded carbon nanotubereinforced composite plate using theory of elasticity. Compos Struct.;106:873-81.
[33] Alibeigloo A. (2013), Static analysis of functionally graded carbon nanotube-reinforced composite plate embedded in piezoelectric layers by using theory of elasticity. Compos Struct.;95:612-22.
[34] M. Mohammadimehr, M. Salemi, B. Rousta Navi (15 March 2016), Bending, buckling, and free vibration analysis of MSGT microcomposite Reddy plate reinforced by FG-SWCNTs with temperature dependent material properties under hydro-thermo-mechanical loadings using DQM, Composite structures, Volume 138, Pages 361–380.
[35] Zhang, L.W., Song, Z.G., Liew, K.M. (15 December 2015), State-space Levy method for vibration analysis of FG-CNT composite plates subjected to in-plane loads based on higher-order shear deformation theory, Composite Structures, Volume 134, Pages 989-1003.
[36] Zhang, L.W., Lei, Z.X., Liew, K.M.(February 2015), Free vibration analysis of functionally graded carbon nanotube-reinforced composite triangular plates using the FSDT and element-free IMLS-Ritz method, CompositeStructures, Volume 120, Pages 189-199.
[37] Shen H S and Zhang C L (2010), Thermal buckling and postbuckling behavior of functionally graded carbon nanotube-reinforced composite plates Mater. Des. 31 3403-3411.
[38] Z.X. Lei , K.M. Liew , J.L. Yu (2013), Buckling analysis of functionally graded carbon nanotube-reinforced composite plates using the element-free kp-Ritz method, Composite Structures 98 160–168
[39] Pandya B.N., Kant T. (1988) Finite element analysis of laminated composite plates using higher order displacement model, Composites Science and Technology, Vol32:137–55.
[40] J. N. Reddy. (2004) Mechanics of laminated composites plates and shells, theory and analysis, CRC press, second edition, pg.671-721.
[41] Zhu J, Yang J and Kitipornchai S (2013), Dispersion spectrum in a functionally graded carbon nanotube-reinforced plate based on first-order shear deformation plate theory Compos. Part B 53 274-283.

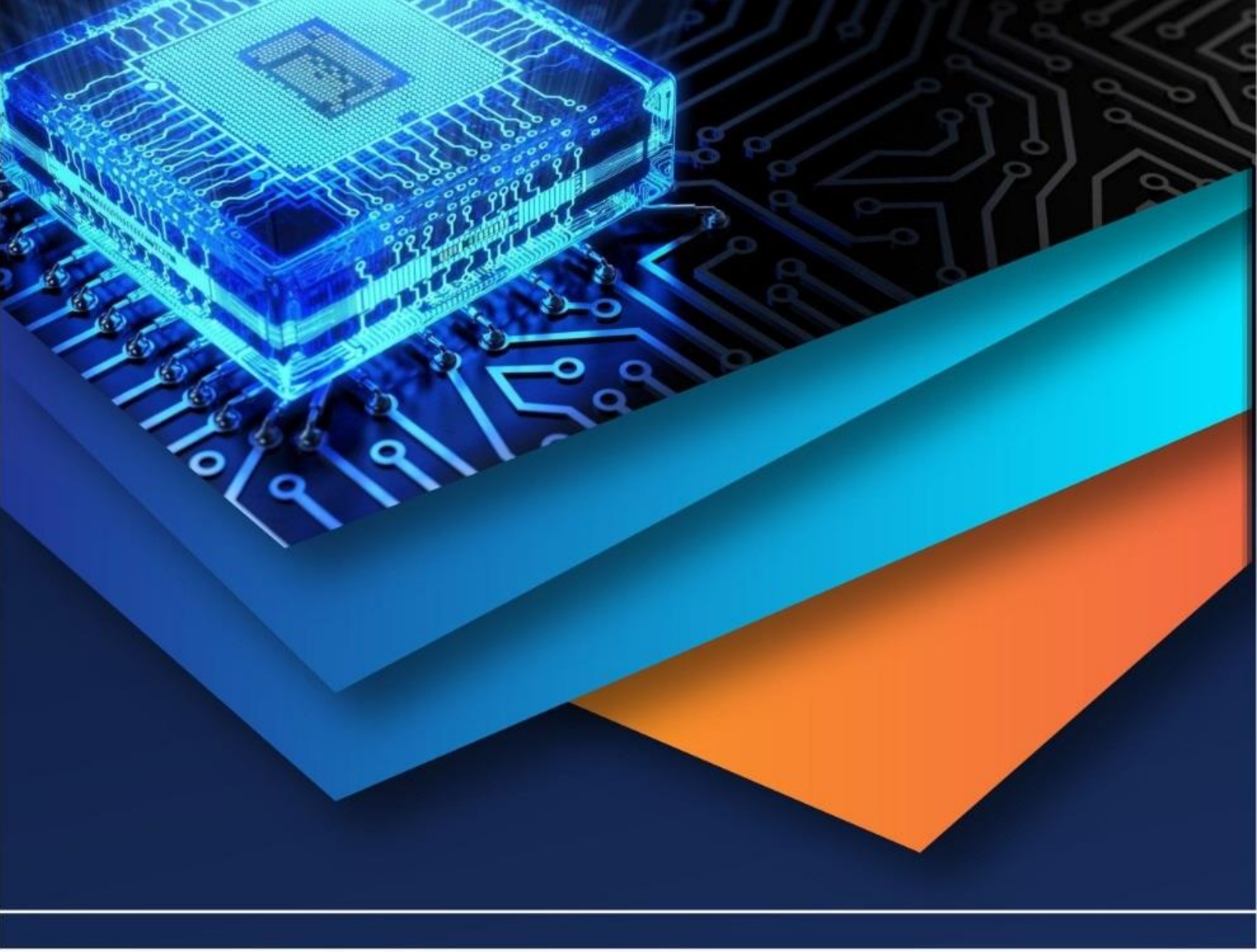

10.22214/IJRASET

45.98

IMPACT FACTOR: 7.129

IMPACT FACTOR: 7.429

INTERNATIONAL JOURNAL FOR RESEARCH

IN APPLIED SCIENCE & ENGINEERING TECHNOLOGY